Cryptotanshinone inhibits lung tumorigenesis and induces apoptosis in cancer cells *in vitro* and *in vivo*

LIANG CHEN[1], HUI-JUAN WANG[2], WENLI XIE[3], YUNYI YAO[4], YAN-SHAN ZHANG[5] and HUILING WANG[1]

[1]Department of Respiratory Medicine, The Second Affiliated Hospital of Dalian Medical University, Dalian Medical University, Dalian, Liaoning 116023; [2]Department of Tumor Chemotherapy, Wuwei Tumor Hospital, Wuwei, Gansu 733000; [3]Department of Cardiology, The Second Affiliated Hospital of Dalian Medical University, Dalian Medical University, Dalian, Liaoning 116023; [4]Research Center for Biochemistry and Molecular Biology, Xuzhou Medical College, Xuzhou, Jiangsu 221004; [5]Department of Tumor Surgery, Wuwei Tumor Hospital, Wuwei, Gansu 733000, P.R. China

Received August 14, 2013; Accepted March 4, 2014

DOI: 10.3892/mmr.2014.2093

Abstract. Cryptotanshinone is one of the compounds extracted from the root of *Salvia miltiorrhiza Bunge*. Unlike other tanshinones, only a small number of studies have focused on cryptotanshinone for medical treatment. In the present study, the A549 lung cancer cell line and xenograft models of human lung tumors were used to assess the anti-cancer effect of cryptotanshinone. The effect of cryptotanshinone on human lung cancer, including growth inhibition, cell cycle arrest and apoptosis factors, were identified *in vitro,* and inhibition of tumor formation, improvement of body condition as well as pathological apoptotic effects were detected *in vivo*. These results suggested that cryptotanshinone is a potential drug for the treatment and prevention of human lung cancer.

Introduction

The root of *Salvia miltiorrhiza Bunge* (S. Bunge), a perennial plant in the Salvia genus, is highly valued in traditional Chinese Medicine. The most effective compounds for medical treatment extracted from the root of S. Bunge are several tanshinone derivatives, including tanshinones I, IIA and IIB, dihydrotanshinone and cryptotanshinone (1). Previous studies mainly focused on the pharmacological effects of tanshinones I and IIA; however, rarely on cryptotanshinone. Tanshinones I and IIA are diterpene quinones exerting anti-inflammatory, anti-oxidative, cytotoxic, apoptosis-inducing and growth-inhibitory effects on numerous types of cancer cells, including human gastric (2), hepatocellular (3), breast (4), and cervical cancer cells (5). Given that cryptotanshinone is structurally homologous to tanshinones I and IIA, their pharmacological effects may be similar. In the present study the anticancer effect of cryptotanshinone on human lung cancer, was assessed *in vitro* and *in vivo*, investigating the pharmacological effects and potential clinical use of cryptotanshinone.

Materials and methods

Drug treatments and assessment of cytotoxic effects. Cryptotanshinone was purchased from LKT Laboratories, Inc. (St. Paul, MN, USA). The human A549 lung adenocarcinoma epithelial cell line was propagated at 37˚C with 5% CO_2 in Roswell Park Memorial Institute (RPMI)-1640 cell culture medium (GIBCO-BRL, Carlsbad, CA, USA) supplemented with L-glutamine, 100 U/ml penicillin, 100 μg/ml streptomycin, and 10% (v/v) fetal bovine serum (FBS; GIBCO, USA). A549 cells ($5x10^3$ cells/well) were seeded in a 96-well plate (Corning, Acton, MA, USA). Cells were treated with cryptotanshinone dissolved in 0.1% DMSO at final concentrations of 1, 5, 20 and 50 μM for 24, 36 and 48 h, respectively. The control group was treated with 0.1% DMSO. The MTT assay was performed to investigate cell growth inhibition and cytotoxicity. The colony-forming assay was performed to assess cell survival following treatment with cryptotanshinone. A549 cells (n=250 were seeded in a 35 mm tissue culture dish (Corning) and allowed to attach overnight prior to treatment with 1, 5, 20 and 50 μM of cryptotanshinone dissolved in DMSO or 0.1% DMSO (control), incubated for 10 days. The colonies were stained with 0.5% crystal violet in methanol/acetic acid (3:1) and those composed of >50 cells were counted. Experiments were performed three times in duplicate.

Cell cycle and analysis of associated genes. According to previous studies, a final cryptotanshinone concentration of 20 μM is the ideal concentration for *in vitro* experiments. A549 cells were seeded in a 6-well plate (Corning) at a density

Correspondence to: Dr Yan-Shan Zhang, Department of Tumor Surgery, Wuwei Tumor Hospital, 31 Weisheng St., Haizang Rd., Wuwei, Gansu 733000, P.R. China
E-mail: zhang-yanshan@163.com

Professor Huiling Wang, Department of Respiratory Medicine, The Second Affiliated Hospital of Dalian Medical University, Dalian Medical University, 467 Zhongshan Rd., Dalian, Liaoning 116023, P.R. China
E-mail: whl882728@163.com

Key words: cryptotanshinone, lung tumorigenesis, tumor inhibition, cell cycle, apoptosis, regulation factor

of $1x10^5$/ml and treated at a final cryptotanshinone concentration of 20 μM for 24 h. Cells were trypsinized, centrifuged (4˚C, 800 g/min, 10 min), washed with phosphate-buffered saline (PBS) and fixed with cold 70% ethanol/30% PBS at 4˚C overnight. Cells were digested by 1,000 units RNase A (Invitrogen, Carlsbad, CA, USA), and then stained with 1% propidium iodide (Sigma, St. Louis, MO, USA) at 37˚C for 30 min. The DNA profiles were determined within 4 h of staining by flow cytometry (FCM; BD FACSArray™, BD Biosciences, Franklin Lakes, NJ, USA). The expression of cell cycle and apoptosis-associated genes was tested using Cell Cycle PCR Array (PAHS-020Z, SABiosciences, Quiagen, Hilden, Germany). The value of the control group was set as 1 while the relative values for the cryptotanshinone group were calculated in correlation with the control group. Significant changes (>2- or <0.5-fold) in the levels of G_2/M cell cycle-associated genes were shown.

Western blot analysis of cell cycle and apoptosis. Total protein extracted (40 μg) from A549 cells treated with cryptotanshinone at a final concentration of 20 μM for 48 h was boiled with 4X loading buffer at 100˚C for 5 min prior to injection in a 12.5% SDS-PAGE. Following electrophoresis and transfer, the polyvinylidene fluoride (PVDF) membrane (Invitrogen, USA) was blocked in 5% non-fat milk for 1 h, incubated overnight at 4˚C with B-cell lymphoma 2 (Bcl2) rabbit polyconal immunoglobulin G (IgG) (1:1000; Signalway Antibody LLD, College Park, MD, USA), Bcl2-associated X (Bax) rabbit polyconal IgG (1:1000; Signalway Antibody), p53 rabbit polyconal IgG (1:1200; AnboBio, San Francisco, CA, USA), cyclin-dependent kinase inhibitor 1A [p21(CIP1/WAF1)], cyclin B1 and cell division cycle 25C (Cdc25C) rabbit polyconal IgG (1:800; Cell Signaling Technology, Inc., Danvers, MA, USA), or cyclin D kinase 1 (CDK1) rabbit polyconal IgG, (1:1000; Merck Millipore, Billerica, MA, USA). Cells were then washed with 1X Tris-PBS, incubated with the secondary antibody [goat anti-rabbit IgG-horseradish peroxidase (HRP), Santa Cruz Biotechnology, Inc., Santa Cruz, CA, USA] for 1 h at room temperature, washed and exposed. β-actin was used as the native control. Images were captured on Kodak film (Kodak, Rochester, NY, USA) for analysis. The value (target protein/β-actin) in the control group was set as 1 while the relative values for the cryptotanshinone group were calculated in correlation with the control group.

Generation and measurement of tumor xenograft mice. Human lung tumor tissue (patient consent was obtained from the patient's family, provided by Wuwei Tumor Hospital) was cut into 3x3x3 mm^3 sections in RPMI-1640 (Gibco) and then subcutaneously injected into the right lower limbs of 24 male nude mice (50 days old; weight, ~18 g, provided by the Animal Research Center, Lanzhou University, China) kept under specific pathogen-free conditions at 24±2˚C and 55±15% humidity. Seven days post-xenotransplantation, the mice with tumor sizes >150 mm^3 were used. Half of these nude mice were subcutaneously injected with 100 μg/g cryptotanshinone per day around the xenotransplantation area for a total of 20 days, according to our previously established method (6). The body weight and tumor size of the nude mice were measured every two days following treatment with cryptotanshinone. Mice with weight loss of >40% or tumor sizes of >2,000 mm^3 were sacrificed according to the animal welfare requirements. Tumor sizes were calculated as $V=\pi/6 \times a \times b^2$ where a is the major and b, the minor axis. Mice were sacrificed by CO_2 inhalation for 3 min. The present study was approved by the Medical Ethics Committee of Wuwei Tumor Hospital, Gansu, China.

Hematoxylin and eosin (H&E) staining, terminal dioxynucleotidyl transferase deoxyuridine triphosphate nick end-labeling (TUNEL) and immunohistochemistry (IHC) detection. Lung tumors transplanted into nude mice were collected on the 20th day and subjected to pathological detection and assessment of apoptosis. Briefly, 4 μm tumor sections were deparaffinized by treatment with fresh xylene as well as 100, 95 and 70% alcohol for 3 min, which was repeated once. The sections were stained in Harris hematoxylin solution for 5 min, differentiated in 1% acid alcohol for 30 sec, blued in 0.2% ammonia water for 30 sec, stained with eosin-phloxine solution for 1 min and then dehydrated with 95 and 100% alcohol as well as xylene for 3 min, which was repeated once. TUNEL detection for apoptosis analysis of 4 μm paraffin sections was performed using the QIA33 FragEL™ DNA Fragmentation Detection kit (Merck KGaA, Darmstadt, Germany) according to the manufacturer's instructions. Paraffin sections (4 μm) were prepared and stained with Bcl2 rabbit polyclonal IgG (1:200; Signalway Antibody), Bax rabbit polyconal IgG (1:200), p53 rabbit polyconal IgG (1:300; Anbobio) and caspase 3 rabbit polyconal IgG (1:200; Cell Signaling Technology) to assess apoptosis in lung tumor tissue following the protocol (Nikon TE2000; Nikon, Tokyo, Japan).

Data analysis. In the present study, all experiments were performed at least three times, both *in vitro* and *in vivo*. Data were presented as the mean ± standard deviation. Calculation and analysis were performed using SPSS 13.0 (USA). These results were evaluated by the Student's t-test (two groups) or one-way ANOVA (multiple groups). A significant difference was defined as $P<0.05$ and $P<0.01$.

Results

Cell growth and colonogenic survival inhibition. As shown in Fig. 1A, cryptotanshinone exerted a dose-dependent cytotoxic effect on A549 cells. Compared with the control group, 1 μM cryptotanshinone showed no obvious growth inhibitory effect within 48 h; however, an effect was observed within 72 h. The growth and viability of A549 cells treated with cryptotanshinone for 24-72 h were significantly inhibited at concentrations >5 μM. No obvious improvement of the inhibitory effect was observed at >20 μM. These results indicate that cryptotanshinone is cytotoxic to A549 cells and thus inhibits cancer cell growth. In the presence of cryptotanshinone at concentrations >5 μM, colony formation of A549 cells was significantly inhibited, while 1 μM cryptotanshinone showed no obvious inhibition effect in the clonogenic assay (Fig. 1B). Both the cell growth and clonogenic survival inhibition study indicated that cryptotanshinone was able to inhibit the growth of A549 cells and 20 μM served as an ideal concentration for subsequent experiments.

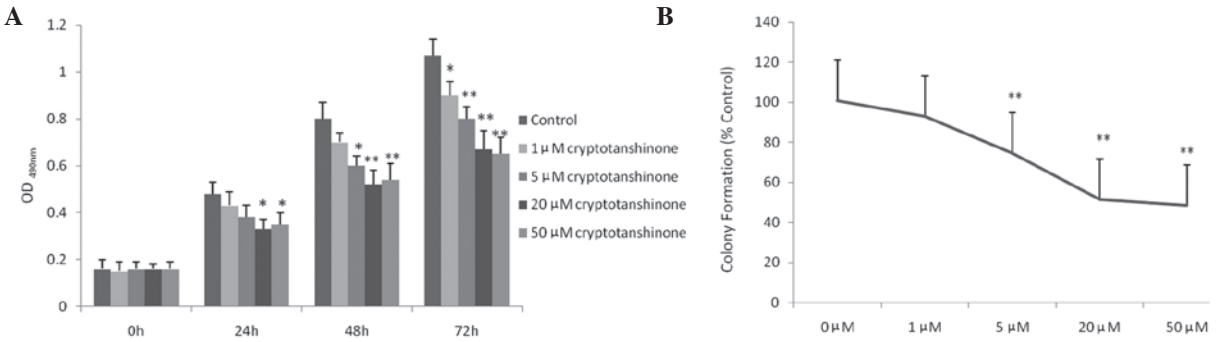

Figure 1. (A) Dose-dependent cytotoxic effect of cryptotanshinone on A549 cells. Compared with the control group, 1 μM cryptotanshinone showed no obvious inhibitory effect on cell growth within 48 h, however, some effect was observed within 72 h. The growth and viability of A549 cells treated with cryptotanshinone for 24-72 h were significantly inhibited at concentrations >5 μM. The increase in activity ceased to increase at concentrations >20 μM. (B) Colony-forming assay for cell survival detection. Clonogenic survival of A549 cells treated with cryptotanshinone at concentrations >5 μM was significantly inhibited, while 1 μM cryptotanshinone showed no obvious inhibitory effect. A significant difference was defined as P<0.05 (*) and P<0.01 (**).

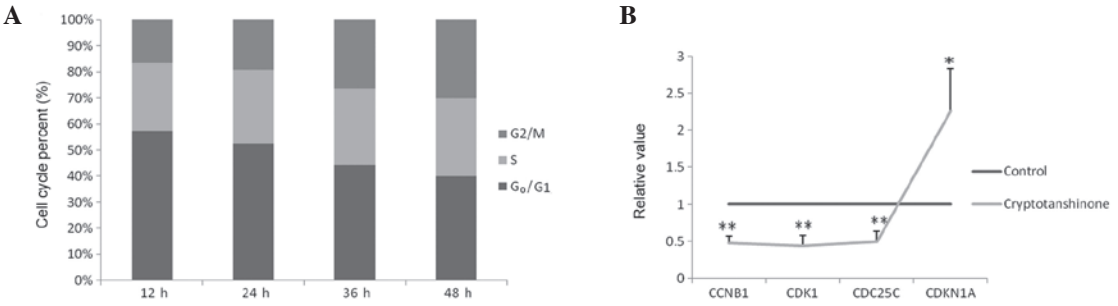

Figure 2. (A) Cell cycle analysis by flow cytometry. Following treatment with 20 μM cryptotanshinone, the percentage of A549 cells in G_0/G_1 phase was decreased while that in G_2/M phases was increased. Cryptotanshinone was able to cause G_2/M phase arrest in A549 cells. (B) G_2/M phase-associated genes were detected using quantitative polymerase chain reaction. CCNB1 (cyclin B1), CDK1 and Cdc25C were downregulated (<0.5-fold) while the expression of CDKN1A (p21CIP1/WAF1) was upregulated (>2-fold). No obvious changes were detected in levels of G_2/M phase-associated genes. Significant differences were defined as *P<0.05 and **P<0.01. G_0/G_1; quiescent phase/growth phase 1; S, DNA synthesis phase; G_2/M, growth phase 2/mitosis phase; CCNB1; cyclin B1; CDK1; cyclin D kinase 1; Cdc25C, cell division cycle 25C; CDKN1A (p21CIP1/WAF1), cyclin-dependent kinase inhibitor 1A.

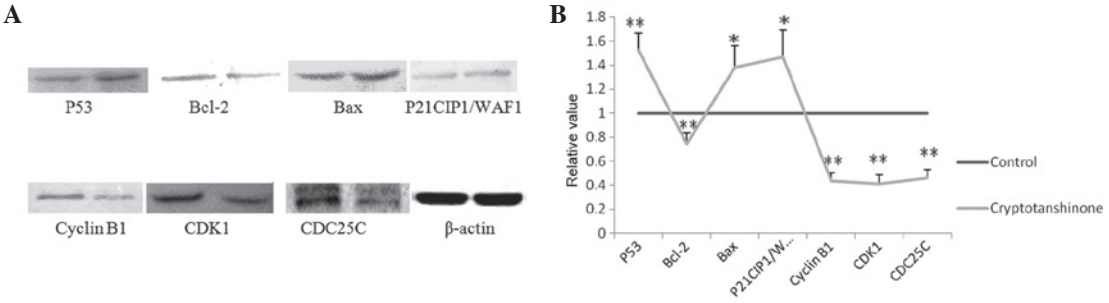

Figure 3. (A) Expression of G_2/M phase-associated proteins cyclin B1, CDK1 and CDC25C were downregulated, while p21CIP1/WAF1 was upregulated following treatment with 20 μM cryptotanshinone, indicating that cryptotanshinone was able to cause G_2/M-phase arrest. The expression of Bcl-2 was downregulated while p53 and Bax were up-regulated following treatment with 20 μM cryptotanshinone, indicating cryptotanshinone was able to induce and promote apoptosis of A549 cells (left, control group; right, cryptotanshinone group). (B) Data analysis for the relative value of protein expression. A significant difference was defined as *P<0.05 and **P<0.01. Bcl-2, B-cell lymphoma 2; Bax; Bcl-2 associated X; p21CIP1/WAF1, cyclin-dependent kinase inhibitor 1A; CDK1; cyclin D kinase 1; Cdc25C, cell division cycle 25C; G_2/M, growth phase 2/mitosis phase.

Cell cycle and analysis of associated genes. As shown in Fig. 2A, compared with the control group, the percentage of cells in G_0/G_1 phase was decreased following treatment with 20 μM cryptotanshinone, while the percentage in the G_2/M phases increased, indicating that cryptotanshinone was able to cause growth arrest in A549 cells at the G_2/M phase. Based on this knowledge, G_2/M phase regulatory genes were assessed. Cyclin B1, CDK1 and Cdc25C were downregulated (<0.5-fold), while the expression of p21(CIP1/WAF1) was upregulated (>2-fold) according to quantitative polymerase chain reaction (qPCR). For other G_2/M phase regulatory genes, no obvious changes were detected. Data are presented in Fig. 2B.

Western blot analysis. As shown in Fig. 3A, the expression of the G_2/M phase-associated proteins cyclin B1, CDK1 and

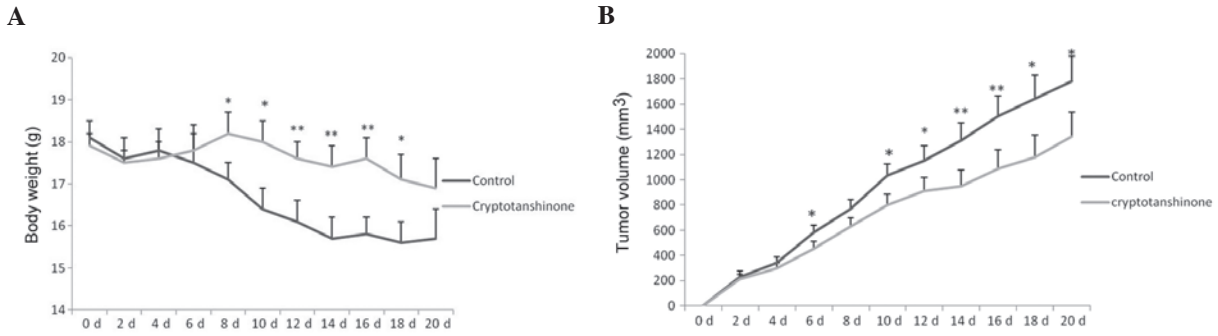

Figure 4. (A) Tumor size in control and cryptotanshinone groups. Without any treatment, tumors grew rapidly. The tumor size was decreased less rapidly in the cryptotanshinone group following treatment at 100 μg/g. (B) Body weight of nude mice decreased rapidly in the control group as compared with the cryptotanshinone group (100 μg/g) due to the inhibition of tumor growth. A significant difference was defined as *P<0.05 and **P<0.01.

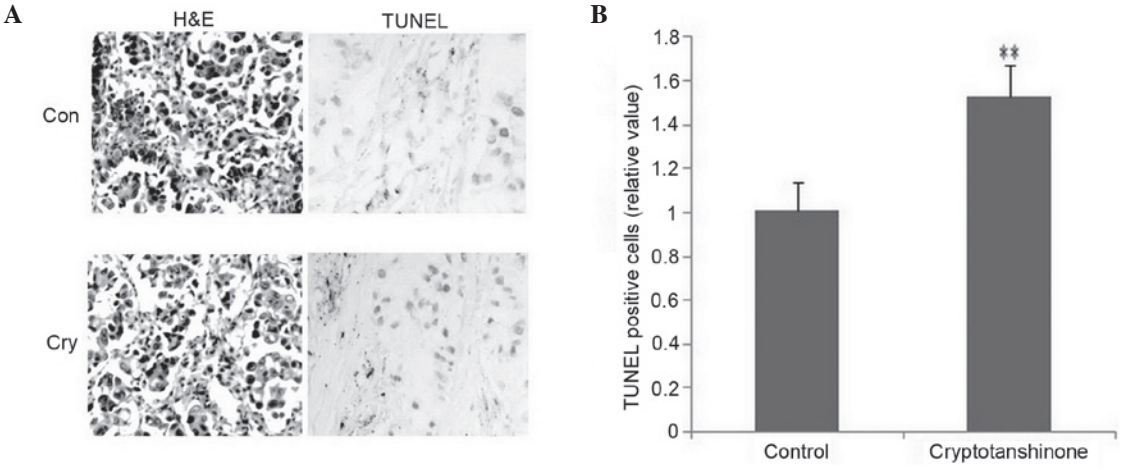

Figure 5. (A) Pathological and apoptotic analysis. Left, H&E staining; right, TUNEL staining. Compared with the control group (Con, upper panel), decreased cancer cell growth and increased apoptosis cells were detected in the cryptotanshinone group (Cry, lower panel) which indicates enhanced apoptosis in the tumor (magnification, x100). (B) Data analysis for the relative value of apoptotic cells. A significant difference was defined as **P<0.01. H&E, hematoxylin and eosin; TUNEL, terminal deoxynucleotidyl transferase deoxyuridine triphosphate nick end-labeling.

CDC25C was downregulated, while p21(CIP1/WAF1) was upregulated following treatment with 20 μM cryptotanshinone, which was in accordance with the results of the qPCR analysis. This result indicated that cryptotanshinone was able to cause cell cycle arrest at the G_2/M phase of A549 cells both at the gene and the protein level. Concerning apoptosis-associated proteins, the expression of Bcl-2 was downregulated, while p53 and Bax were upregulated following treatment with 20 μM cryptotanshinone. This result indicated that cryptotanshinone was able to induce and promote the apoptosis of A549 cells (Fig. 3B).

Analysis of body weight and tumor size of xenografts. As shown in Fig. 4A, the tumor in the control group exhibited rapid growth. Tumors with uncontrolled growth require large amounts of nutrition, and thus, weaken the animals' bodies. However, the tumor size in the xenografts decreased gradually in the cryptotanshinone group compared with the control group. As shown in Fig. 4B, due to the rapid growth of the tumors and their use of nutrition, the body weight of the animals decreased rapidly in the control group. These animals appeared to be weak due to bearing large tumors. However, the body weight in the cryptotanshinone group decreased less rapidly compared with the control group due to the inhibition of tumor growth. The physical and mental condition of the animals in the cryptotanshinone group appeared to be improved as compared to the control group. The present study results indicate that cryptotanshinone was not only able to inhibit the growth of human lung cancer *in vivo*, but also improve the physical and mental status of tumor-bearing mice.

Assessment of apoptosis in xenograft tumors. The inhibition of tumor growth was caused and promoted by apoptosis. As shown in Fig. 5A (left), compared with the cryptotanshinone group, a larger number of abnormal hyperplasia with abundant cytoplasm, irregularities with pleomorphic nuclei and crude chromatin granules were detected for epithelial cells in the control group, accompanied by infiltration of inflammatory cells using H&E staining for pathological detection. As shown in Fig. 5A (right), an increased number of apoptotic cells was detected in the cryptotanshinone group using a TUNEL kit. These increased positive cells indicated enhanced apoptosis following treatment with cryptotanshinone. Data were analyzed in Fig. 5B for TUNEL detection. IHC was used to detect apoptotic key factors *in situ*. As

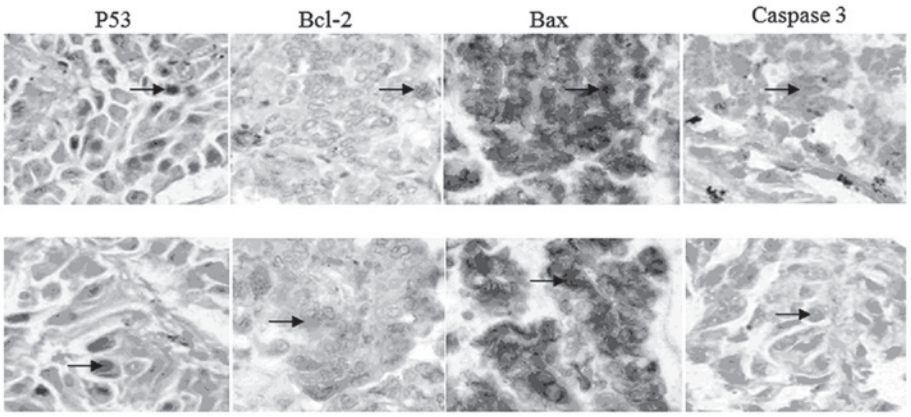

Figure 6. IHC detection for key factors of apoptosis. P53 (nuclear staining, indicated by arrow), Bax (cytoplasm staining, indicated by arrow) and caspase 3 (nuclear staining, indicated by arrow) were increased, while Bcl-2 (cytoplasm staining, indicated by arrow) was decreased in the cryptotanshinone group (Cry, lower panel) compared with the control group (Con, upper panel). H&E, TUNEL, magnification, x100; IHC, magnification, x400). IHC, immunohistochemistry; H&E, hematoxylin and eosin; TUNEL, terminal deoxynucleotidyl transferase deoxyuridine triphosphate nick end-labeling. Bcl-2, B-cell lymphoma 2; Bax; Bcl-2 associated X.

shown in Fig. 6, p53 (nuclear staining, indicated by arrow) was increased, Bcl-2 (cytoplasmic staining, indicated by arrow) was decreased, Bax (cytoplasmic staining, indicated by arrow) was increased, caspase 3 (nuclear staining, indicated by arrow) was increased in the cryptotanshinone group compared with the control. The present study indicated that cryptotanshinone was able to promote apoptosis in human lung cancer xenografts and inhibit the growth of tumors *in vivo*. The key factors involved in this process are p53, Bax/Bcl2 and caspase 3. This result was in accordance with the western blot analysis and supported the conclusion thereof.

Discussion

Lung cancer is a leading cause of cancer mortality in China. An increasing number of people, particularly adult men, die from lung cancer more than from any other type of cancer. Lung cancer is caused by uncontrolled cell growth in the lung, then spreads to nearby tissue in metastasis, and eventually, to other parts of the body. Lung cancer includes small-cell lung carcinoma (SCLC) and non-small-cell lung carcinoma (NSCLC). The identification of new anti-lung cancer drugs is highly important. Cryptotanshinone, together with tanshinones I, IIA, IIB and dihydrotanshinone, are the most abundant constituents of the root of *Salvia miltiorrhiza*, a perennial plant of the Salvia genus, which is highly valued for its roots in traditional Chinese Medicine. Most studies focused on the antioxidant and anti-inflammatory effects (7) of tanshinone I and IIA, which exert an anti-cancer effect (8). However, to the best of our knowledge, cryptotanshinone has rarely been studied.

The growth inhibition of human lung cancer cells by cryptotanshinone was investigated using the MTT assay and the clonogenic survival inhibition was assessed. The results indicated that cryptotanshinone exerted a dose-dependent cytotoxic effect on A549 cells. Concentrations of cryptotanshinone >5 μM showed the significant inhibition of cell growth and clonogenic survival; however, no obvious improvement was observed >20 μM. Cell growth and clonogenic survival are regulated by the cell cycle. The cell cycle is a series of events leading to cell division and duplication, which consists of four distinct phases: G_1 phase, S phase (synthesis), G_2 phase (interphase) and M phase (mitosis). The cell cycle is controlled by checkpoints that ensure the fidelity of cell divisions in eukaryotic cells (9). The first checkpoint is situated at the end of the G_1 phase and the second checkpoint at the end of the G_2 phase (10). The cell cycle analysis performed in the present study using FCM showed that cryptotanshinone was able to cause G_2 phase arrest in A549 cells, indicated by an increased percentage of cells in G_2/M and decreased percentage of cells in G_0/G_1. This triggers the start of the M phase (mitotic phase), thus inhibiting cancer cell growth. The cell cycle is driven by cyclin-dependent kinases (CDK) associated with cyclins. It was then attempted to identify the regulators of the observed G_2 phase inhibition. The expression of G_2/M-associated cyclin B/CDK1 and Cdc25C was observed, together with cyclin-dependent kinase inhibitor (CKI) p21(CIP1/WAF1) (11). The results indicated that following treatment with cryptotanshinone, the expression of cyclin B1, CDK1 and Cdc25C was downregulated at the gene and the protein level, while p21 was upregulated. Accumulation of cyclin B increases the activity of CDK1 prior to entering mitosis, which has a key role in the regulation of cell division. The Cdc25 phosphatase family regulates the dephosphorylation of cyclin B/CDK1 and triggers entry into mitosis, together with the suppression of p53-induced growth inhibition (12). p21(CIP1/WAF1) acts as a regulator of cell cycle progression, controlled by the tumor suppressor protein p53. Growth arrest by p21 is able to promote cell differentiation and death, preventing cell proliferation (13).

Xenografts are effective models for assessing the effect of compounds on the formation and growth of tumors, and are widely used in pre-clinical studies. The tumor size and body weight are the most important data. In the present study, the body weight of the nude mice was decreased in the control group due to the rapid growth of the tumor. These animals appeared to be weak as a portion of their nutrition was used by the tumor. Following treatment with cryptotanshinone, the body weight of the nude mice was decreased less rapidly than in the control, together with an improved physical and

mental condition. Without any treatment, the tumor size increased rapidly. The uncontrolled growth of the tumor used up the nutrition and emaciated the mice. The tumor size decreased less rapidly in the cryptotanshinone group. The present study indicated that cryptotanshinone was able to inhibit the growth of human lung tumors in an *in vivo* model. Tumor growth occurs due to numerous reasons, of which an important one is the imbalance of cell proliferation and cell death pathways. Over-expression of anti-apoptotic factors, and under-expression of pro-apoptotic factors may lead to increased proliferation and lack of cell death, resulting in cancer. In the present study, an increased number of abnormal hyperplasia with abundant cytoplasm, irregularities and pleomorphism of the nucleus, crude chromatin granules were detected for epithelial cells in the control group, accompanied by infiltration of inflammatory cells to a greater extent than in the cryptotanshinone-treated group using H&E staining for pathological detection. The present study indicated that cryptotanshinone arrested tumor growth. Apoptosis, also known as programmed cell death (PCD), is a series of biochemical events leading to morphological changes, which include blebbing, cell shrinkage, nuclear fragmentation, chromatin condensation, chromosomal DNA fragmentation and finally cell death (14). Apoptosis of cancer cells, controlled by a diverse range of cell signals, is considered as an efficient method for cancer treatment (15). Numerous key regulators are involved in apoptosis, among which p53, Bcl-2 and members of the caspase family are most important. Bcl-2 family members share one or more of the four characteristic domains (BH1, BH2, BH3 and BH4), and thus form hetero- or homodimers, acting as anti-[Bcl-2, b-cell lymphoma extra large (Bcl-xl) and Mcl1] or pro-apoptotic (Bax) regulators (16). Following induction of apoptosis, Bax may be involved in p53-mediated apoptosis, and induce the opening of the mitochondrial voltage-dependent anion channel, releasing cytochrome c and other pro-apoptotic factors from the mitochondria (17,18), leading to the activation of caspases, among which caspase 3 is the key factor (19). The expression of Bax was upregulated by the tumor suppressor protein p53. Bcl-2 had the opposite role during this process (20). The present study revealed that cryptotanshinone enhanced the expression of p53 and Bax and downregulated the expression of Bcl-2 both *in vitro* and *in vivo*, which suggested that cryptotanshinone induced apoptosis in cancer cells. Cryptotanshinone activated caspase 3 *in vivo*, indicating that this apoptosis may be caspase-mediated.

In conclusion, the present study has demonstrated that cryptotanshinone causes growth-inhibition, cell cycle arrest, apoptosis and inhibition of tumor formation in human lung cancer both *in vitro* and *in vivo*. These results suggest that cryptotanshinone is a potential compound for the treatment and prevention of human lung cancer. Future studies on the anti-cancer effect of cryptotanshinone should be conducted.

Acknowledgements

The present study was supported by the research program of of Wuwei Tumor Hospital Research Program and Jiangsu Provincial Natural Science Foundation (BK20130219).

References

1. Wang JW and Wu JY: Tanshinone biosynthesis in *Salvia miltiorrhiza* and production in plant tissue cultures. Appl Microbiol Biotechnol 88: 437-449, 2010.
2. Xu M, Cao FL, Li NY, Liu YQ, Li YP and Lv CL: Tanshinone IIA reverses the malignant phenotype of SGC7901 gastric cancer cells. Asian Pac J Cancer Prev 14: 173-177, 2013.
3. Yuxian X, Feng T, Ren L and Zhengcai L: Tanshinone II-A inhibits invasion and metastasis of human hepatocellular carcinoma cells in vitro and in vivo. Tumori 95: 789-795, 2009.
4. Nizamutdinova IT, Lee GW, Son KH, Jeon SJ, Kang SS, Kim YS, Lee JH, Seo HG, Chang KC and Kim HJ: Tanshinone I effectively induces apoptosis in estrogen receptor-positive (MCF-7) and estrogen receptor-negative (MDA-MB-231) breast cancer cells. Int J Oncol 33: 485-491, 2008
5. Pan TL, Hung YC, Wang PW, Chen ST, Hsu TK, Sintupisut N, Cheng CS and Lyu PC: Functional proteomic and structural insights into molecular targets related to the growth inhibitory effect of tanshinone IIA on HeLa cells. Proteomics 10: 914-929, 2010
6. Zhang Y, Yao Y, Wang H, Guo Y, Zhang H and Chen L: Effects of salidroside on glioma formation and growth inhibition together with improvement of tumor microenvironment. Chin J Cancer Res 25: 520-526, 2013.
7. Wang X, Morris-Natschke SL and Lee KH: New developments in the chemistry and biology of the bioactive constituents of Tanshen. Med Res Rev 27: 133-148, 2007.
8. Ma H, Fan Q, Yu J, Xin J and Zhang C: Novel microemulsion of tanshinone IIA, isolated from *Salvia miltiorrhiza* Bunge, exerts anticancer activity through inducing apoptosis in hepatoma cells. Am J Chin Med 41: 197-210, 2013.
9. Heber-Katz E, Zhang Y, Bedelbaeva K, Song F, Chen X and Stocum DL: Cell cycle regulation and regeneration. Curr Top Microbiol Immunol 367: 253-276, 2013.
10. Vleugel M, Hoogendoorn E, Snel B and Kops GJ: Evolution and function of the mitotic checkpoint. Dev Cell 23: 239-250, 2012.
11. Gallorini M, Cataldi A and di Giacomo V: Cyclin-dependent kinase modulators and cancer therapy. BioDrugs 26: 377-391, 2012.
12. Miyazaki T and Arai S: Two distinct controls of mitotic cdk1/cyclin B1 activity requisite for cell growth prior to cell division. Cell Cycle 6: 1419-1425, 2007.
13. Warfel NA and El-Deiry WS: p21WAF1 and tumourigenesis: 20 years after. Curr Opin Oncol 25: 52-58, 2013.
14. Wlodkowic D, Skommer J and Darzynkiewicz Z: Cytometry of apoptosis. Historical perspective and new advances. Exp Oncol 34: 255-262, 2012.
15. Rebucci M and Michiels C: Molecular aspects of cancer cell resistance to chemotherapy. Biochem Pharmacol 85: 1219-1226, 2013.
16. Barillé-Nion S, Bah N, Véquaud E and Juin P: Regulation of cancer cell survival by BCL2 family members upon prolonged mitotic arrest: opportunities for anticancer therapy. Anticancer Res 32: 4225-4233, 2012.
17. Kubli DA and Gustafsson ÅB: Mitochondria and mitophagy: the yin and yang of cell death control. Circ Res 111: 1208-1221, 2012.
18. Monian P and Jiang X: Clearing the final hurdles to mitochondrial apoptosis: regulation post cytochrome C release. Exp Oncol 34: 185-191, 2012.
19. Snigdha S, Smith ED, Prieto GA and Cotman CW: Caspase-3 activation as a bifurcation point between plasticity and cell death. Neurosci Bull 28: 14-24, 2012.
20. Cakir E, Yilmaz A, Demirag F, Oguztuzun S, Sahin S, Yazici UE and Aydin M: Prognostic significance of micropapillary pattern in lung adenocarcinoma and expression of apoptosis-related markers: caspase-3, bcl-2, and p53. APMIS 119: 574-580, 2011.